

The challenges in guided self-assembly of Ge and InAs quantum dots on Si

Z.M. Zhao^a, T.S. Yoon^a, W. Feng^a, B.Y. Li^a, J.H. Kim^a, J. Liu^a, O. Hulko^a, Y.H. Xie^{a,*},
H.M. Kim^b, K.B. Kim^b, H.J. Kim^c, K.L. Wang^c, C. Ratsch^d, R. Caflisch^d,
D.Y. Ryu^e, T.P. Russell^e

^a Department Mat. Sci. & Eng., University of California at Los Angeles, Box 951595, Los Angeles, California 90095-1595, USA

^b School of Materials Science and Engineering, Seoul National University, Seoul 151-742, Korea

^c Department of Electrical Engineering, University of California at Los Angeles, CA 90095, USA

^d Department of Mathematics, University of California at Los Angeles, CA 90095, USA

^e Department of Polymer Science and Engineering, University of Massachusetts, Amherst, Massachusetts 01003, USA

Available online 18 November 2005

Abstract

The topic of guided self-assembly of Ge and InAs quantum dots on Si (001) substrates via epitaxy is discussed. A buried misfit dislocation network can be used to guide the assembly process through the associated strain field. Patterned substrates can also be used to guide the assembly process. This paper discusses the recent experimental and theoretical studies of the guided assembly process with an emphasis on what remains to be understood.

© 2005 Elsevier B.V. All rights reserved.

Keywords: Ge; InAs; Quantum dots; Self-assembly

1. Introduction

Driven by the need for applications of novel electronic and optoelectronic devices, the subject of self-assembly of semiconductor quantum dots (SAQDs) via epitaxy has been actively pursued over the last decade [1–6]. More recently, the research efforts have been focusing on the subject of guided assembly, in which the assembly processes of the quantum dots are guided by either undulating strain fields or patterned topographic features on the substrate surface [7,5]. The underlying mechanism for the guided assembly processes, while seemingly intuitively obvious, remains poorly understood.

This paper presents some of the recent results on the subject of guided assembly of materials combinations including Ge on Si (001) and InAs on Si (001), with emphasis on the poorly understood aspects. The discussion is divided into three parts: stressor-guided assembly, topography-guided assembly and the assembly of chemically incompatible materials, i.e. InAs on Si.

2. Experimental

All Ge on Si Samples used in this study were grown by a Riber EVA-32 molecular beam epitaxy (MBE) system equipped with two electron beam evaporation sources of Si and Ge, respectively. The details of sample cleaning and preparation are described in Ref. [1].

For the stressor-guided assembly study, samples with an 800 Å thick Si_{0.9}Ge_{0.1} buffer layer and a 100 Å thick Si cap layer were grown at 550 °C and 600 °C, respectively. The buffer layer was almost completely strained as grown. Then the samples underwent a post-growth anneal at 700 °C for 30 min that led to the partial strain relaxation of the Si_{0.9}Ge_{0.1} buffer layer via dislocation. The function of the Si cap layer under tensile strain is to preserve a flat surface [8]. The resulting samples consist of an undulating strain field with an atomically flat top surface (RMS on the order of a few angstroms). The quality of the resulting surface was examined using reflection high-energy electron diffraction (RHEED). Streaky (2 × 1) patterns were observed for all samples throughout the growth and annealing processes. Ge SAQDs growths were carried out at 700 °C with Ge coverage ranging from 3.0 to 12.0 Å. All samples employed the slow growth

* Corresponding author. Tel.: +1 310 825 8671; fax: +1 310 206 7353.

E-mail address: yhx@ucla.edu (Y.H. Xie).

rate of 0.05 Å/s. After Ge growths, the samples were quenched to room temperature.

For the topography-guided assembly study, Si (100) substrates having hexagonally ordered hole patterns on the surface were prepared through patterning using diblock copolymer, consisting of two chemically dissimilar polymer chains joined by covalent bonds. We used diblock copolymer of polystyrene-*block*-poly(methylmethacrylate) (PS-*b*-PMMA), which forms the hexagonally organized cylindrical patterns after self-assembly. The detail behavior of self-assembly of PS-*b*-PMMA forming cylindrical patterns was previously reported in detail [9]. The hexagonally organized cylindrical pattern of PS-*b*-PMMA on Si substrates was transferred through reactive ion etching (RIE) with SF₆ etching chemistry, which forms the holes pattern with a lateral size less than 40 nm and depth of about 25 nm on Si substrates. Two-step Ge growth process was employed in which a 0.3 nm thick Ge was first grown at 200 °C and then a 0.6 nm thick Ge was subsequently grown at 600 °C in order to minimize the intermixing between Ge and Si substrate [10].

InAs SAQDs on Si (001) samples were grown on n-type (001) orientated Si substrate in a Perkin-Elmer 430 MBE with an arsenic cracker cell. Si substrates were cleaned using the following recipe: (1) H₂O₂/H₂SO₄ (3:5) 1 min, (2) HF/H₂O (1:10) 1 min. This procedure was repeated three times with the final step being the HF dip, rendering H-terminated Si surface. The substrates were blown dry in nitrogen and immediately loaded into the MBE chamber to preserve the clean H-passivated surface. The background vacuum in MBE chamber was kept at 4×10^{-10} Torr with liquid nitrogen cryo-shield. Before growth, substrates were degassed for 50 min at 250 °C to desorb carbon-containing species. H desorption was carried out at 780 °C until the appearance of a clear 2×1 RHEED pattern. At this point, substrate temperature was ramped down to the growth temperature and InAs was deposited directly on Si. InAs growths were initiated by opening the arsenic shutter 2 min before opening the indium shutter. Substrate temperature 320 °C, InAs growth rate 0.02 ML/s and As beam equivalent pressure 1.4×10^{-6} Torr was used for InAs growth. After growths, samples were removed from the MBE chamber and exposed to the atmosphere without capping.

Planview scanning electron microscopy (SEM, JSM 6700F) and transmission electron microscopy (TEM, JEOL 2000FX with an operating voltage of 200 kV) were used to characterize the samples. Cross-sectional high-resolution TEM (JEM 3000 F operating at 300 kV with a field-emission electron gun) was also used in order to investigate the interface and microstructure of Ge SAQDs. The surface topography was determined using a Park Scientific atomic force microscopy operating in contact mode.

3. Results and discussion

3.1. Stressor-guided assembly of Ge on Si (001)

Preferential nucleation and growth of Ge SAQDs on a surface with a buried misfit dislocation network as shown in

Fig. 1 were observed in 1997 by several research groups [11–13]. The buried dislocation network was introduced via partially relaxed epitaxial SiGe buffer layer grown on Si (001) substrates. It was determined that Ge dots preferentially located along the line defined by the intersection between the slip plane of the buried dislocation and the substrate surface. Fig. 2 shows the planview TEM image with the Burgers vector associated with each misfit dislocation indicated by the arrows. It can be easily calculated that the Ge dots are indeed located near the intersection between the slip plane and the surface. The preferential location of Ge SAQDs persists up to a properly engineered dislocation network; such samples can be used to study in detail the nucleation and growth processes of Ge SAQDs [14].

The reason for Ge SAQDs to preferentially grow along dislocation lines appears to be intuitively obvious, while a closer examination of such reasoning leads to many questions. For example, the finite size of the Ge dots does not allow a precise determination as to whether the dots are located on the compressive or the tensile side of the line of intersection. It is well known that the growth of Ge SAQD on Si proceed via Stranski-Krastanov mode in which misfit strain is the only driving force for dot nucleation. By this reasoning, it is expected that the Ge dots under compression would prefer to nucleate on the compressive side of the line where the required super-saturation of Ge adatoms is the lowest. The actual super-saturation of Ge adatoms, on the other hand, is determined by the chemical potential gradient, which is directly related to the binding energy. Recent progress in *ab initio* calculations allows the binding energies under the various substrate strains to be calculated. The results show that the binding energy is dependent on the chemistry of the surface, i.e. Ge on Si versus Ge on Ge, as well as the direction of the uniaxial strain (which is the case in the vicinity of dislocations) with respect to that of the dimer row [15]. A seemingly simple situation is actually rather complex. Furthermore, the calculated variation of typical binding energy change is on the order of 10–20 meV for each percent of strain. Preferential nucleation of Ge dots on Si has been observed with the depth of the dislocations ranging from 50 nm to 300 nm. For a moderate 100 nm depth of the dislocation network, the magnitude of strain undulation from elasticity calculation is on the order of 0.04%, leading to a

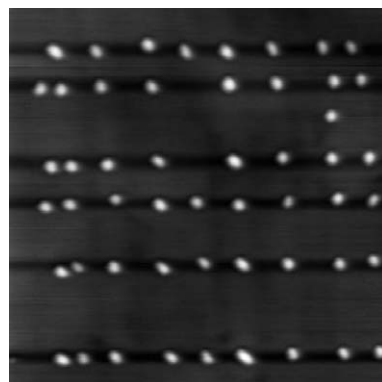


Fig. 1. $2 \mu\text{m} \times 2 \mu\text{m}$ AFM of Ge on Si/SiGe/Si with the SiGe layer being partially relaxed.

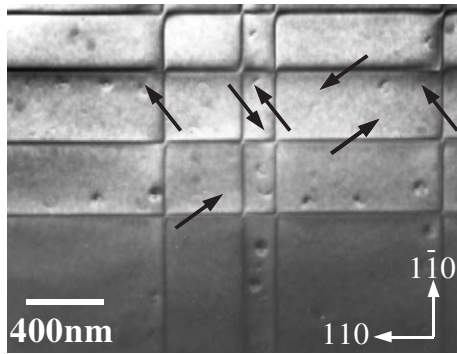


Fig. 2. Planview TEM showing the Burger's vector for each dislocation as well as the relative position of the Ge SAQDs.

binding energy fluctuation of 0.1–0.2 meV. Comparing the thermal energy of $kT \sim 75$ meV at ~ 600 K growth temperature, it is not likely that the 0.1–0.2 meV fluctuation could lead to the distinct preferential nucleation of Ge dots. It is fair to say that this point remains to be understood.

To assess the impact of the undulating binding energy and the resulting diffusion barrier from ab initio calculations, we perform simulation using the level-set method [16]. The results are shown in Fig. 3(a) and (b), corresponding to the two extreme scenarios of varying diffusion barrier with and without the associated chemical potential gradient, respectively. Preferential nucleation can be clearly observed in both cases, though the location in one case is at where the diffusion barrier is the minimum and is the opposite in the other case. In practice, the exact location will depend on the relative values of the chemical potential gradient compared to the change in diffusion barrier height.

Another complication is the decrease in the Ge wetting layer thickness with increasing strain. With a uniform Ge flux, the variation in the wetting layer thickness could lead to a corresponding variation in Ge adatom density. Finally, it has been proposed that the mass migration of Ge could be dominated by the migration of Ge dimers instead of individual adatoms [5]. Any of the above mentioned factors could have

profound impact on the dominant mechanism for Ge SAQD nucleation.

3.2. Topography-guided assembly of Ge on Si (001)

Since the early work by Kamins and Williams [17], many studies have been conducted on the epitaxial growth of Ge SAQDs on patterned Si (001) substrates. It has recently become clear that nucleation depends on the specific layer sequences; Ge dots can be made to nucleate either along the edge of the top surface, on the sidewalls or at the bottom of the patterned mesas. It is proposed that the preferential nucleation is either guided by the elastic relaxation of the Ge wetting layer near the convex portion of the surface [6] or the directional diffusion on slanted surfaces dominated by double layer height steps [18]. While the elastic relaxation of the Ge wetting layer can in principle be calculated, the actual calculation with reasonable level of accuracy falls in the crack between ab initio methods (incapable of taking into consideration of long range elastic effects) and elasticity theory (difficulty in properly account for the surface).

The majority of the experimental studies are carried out on substrate patterned with micrometer size features. The length scale is comparable to the diffusion length of Ge adatoms under typical epitaxial growth conditions. Recently, a new approach employing diblock copolymers has been demonstrated for nano-patterning [4]. GaAs on GaAs homo-epitaxial growths in the absence of misfit strain has been demonstrated. We have begun a systematic study of strained layer epitaxy on diblock copolymer patterned substrates. The initial results from Ge grown on topographically patterned Si using PS-PMMA diblock copolymer is shown in Fig. 4(a) and (b). Ge dots appear to preferentially nucleate near the bottom perimeter of individual holes of ~ 40 nm diameter, ~ 25 nm deep and subsequently grow till the hole is completely filled. There appear to be a kinetic barrier to further increase in the size for individual Ge dots once the hole in the Si substrate is completely filled. Hole filling

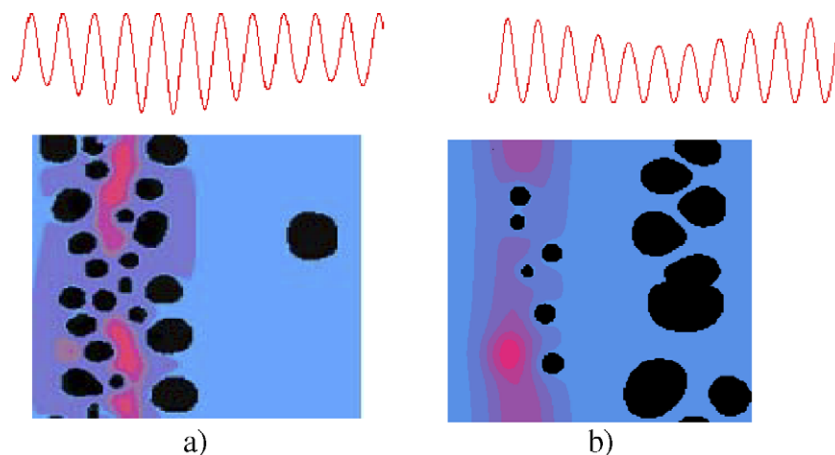


Fig. 3. The results of level set method: (a) with a chemical potential gradient and (b) without a chemical potential gradient. The black patches represents Ge islands. The undulating curves on the top show the undulating potential encountered by Ge adatoms. The difference between the highest and the lowest diffusion barrier heights is assumed to be ~ 250 meV in both (a) and (b).

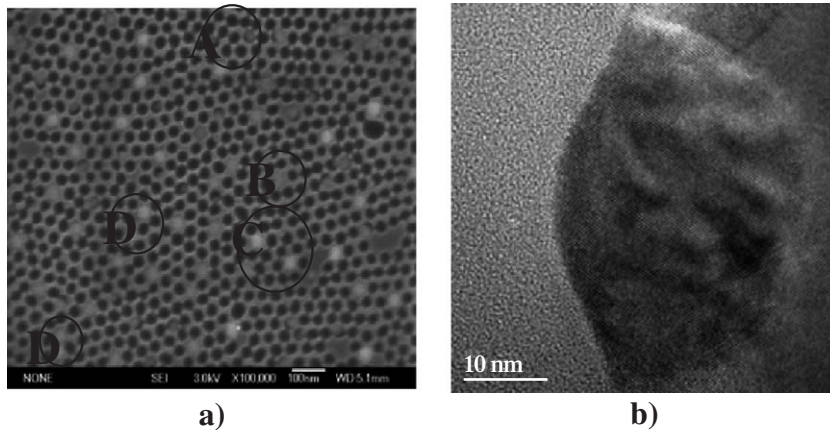


Fig. 4. (a) SEM image of Ge dots grown on copolymer patterned Si (001); (b) XTEM image of one Ge dot grown in a patterned Si pit. 60° dislocations are seen near the substrate interface.

appears to be non-uniform under the experimental condition. Furthermore, 60° dislocations are clearly observed under high resolution (Fig. 4b). Planview Moiré fringe analysis indicates that all of the Ge dots are significantly relaxed, either elastically or plastically via dislocation as in most of the larger dots.

While the initial results did not provide defect free Ge dots, they did show the potential of fabricating high aspect ratio (up to 1:1), high density (up to $5 \times 10^{10} \text{ cm}^{-2}$) and ordered (with hexagonal symmetry) Ge dots on Si. The high aspect ratio and high density cannot be achieved from Ge epitaxially grown on planar Si substrates, which is dictated by the fundamental materials physics governing the Ge on Si material combination.

In addition to Ge growth on topographically patterned Si substrates, we have also carried out growths of Ge on Si substrates patterned using a SiO_2 mask. Fig. 5 is a SEM image of the sample with the SiO_2 mask etched away. In this case, the aspect ratio of individual Ge dots remains low ($\sim 1:5$), but the dot size is uniform and the density is high ($\sim 5 \times 10^{10} \text{ cm}^{-2}$).

The approach of using diblock copolymer to pattern Si substrates for ordered Ge quantum dot fabrication does hold high promise. In the meantime, it also opens up the interesting questions such as the reason for the absence of Ge dots on the flat surface of the patterned Si substrates, and

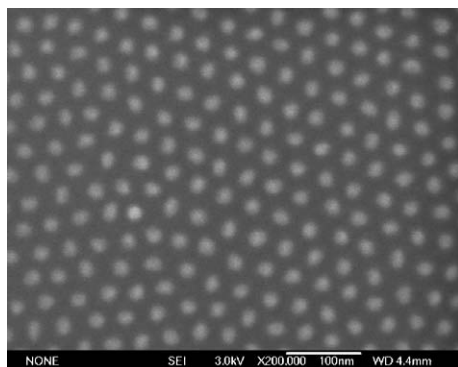


Fig. 5. SEM image of 4 nm Ge grown on SiO_2 mask patterned using diblock copolymer.

the contrast in dot size uniformity between the two different patterning methods. Further study is underway to answer these questions.

3.3. InAs quantum dots grown on Si (001)

The appearance of well-defined islands with InAs coverage below than 1 ML complemented with the typical three-dimensional RHEED pattern provided the indisputable evidence that the growth proceed via Volmer-Weber growth mode. Fig. 6 shows a small InAs island of less than 10 nm in diameter in which dislocation is clearly visible. Lattice parameter calculated from Moiré fringe analysis show that the residual strain is around 1%, which is 10% of the total misfit strain with 90% of the original misfit stain relaxed by misfit dislocations.

Fig. 7 shows the evolution of the InAs island shape with its size. Typical InAs islands go through a pyramidal shape bordered by $\{111\}$ facets that evolve into multiple faceted dome shape with increasing island size.

To examine whether stressor-guided assembly of InAs dots on Si (001) was possible, we grew InAs on the partially relaxed buffer layers described in the stressor-guided assembly of Ge on Si section of this report. For typical depth of ~ 800 nm of the buried dislocation network, no preferential location of InAs was observed. The plastic deformation via dislocation at very small InAs island size may be responsible for the lacking of

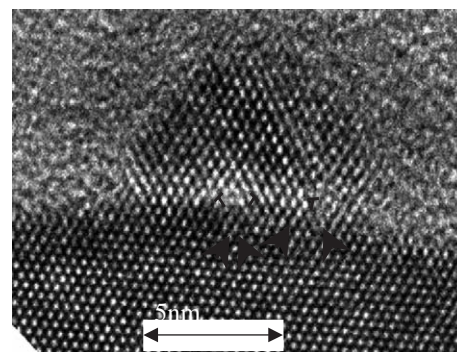


Fig. 6. HRTEM of an individual InAs dot on Si (001). 60° and 90° dislocations are indicated in the figure.

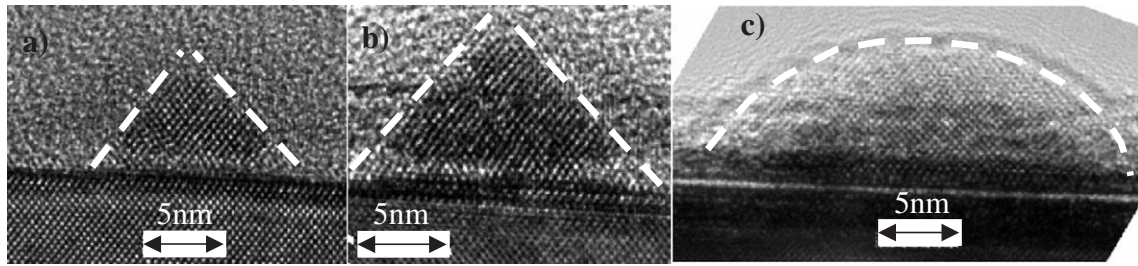


Fig. 7. InAs dot shape evolution and the pyramid to dome transition viewed through HRTEM.

preferential nucleation, but more study is needed to reach a more conclusive understanding.

InAs on Si is interesting largely because of its potential for Si optoelectronics. However, the observed set of dislocation in InAs dots as small as 10 nm makes such application unlikely. The effective band gap, that is the separation between the quantum confined ground states in conduction band and that in valence band, of a 10 nm InAs dots can be extrapolated to be larger than 1.3 eV based on the large collection of InAs SAQD on GaAs (001) data [19]. Considering the Si band gap of 1.1 eV, the effective band gap of InAs QDs of less than 10 nm size precludes the possibility of simultaneous confinement of electrons and holes, i.e. type-I band alignment which is necessary for optoelectronic applications, especially for light emitting applications.

4. Conclusion

This report describes experimental and theoretical studies on the subject of guided assembly via epitaxy. Stressor-guided as well as topography-guided assembly was demonstrated for Ge on Si (001). It remains to be understood whether the binding energy gradient or the diffusion barrier gradient of Ge adatoms is the dominant factor governing the preferential nucleation of Ge dots for both types of guided assembly processes. InAs growth on Si (001) is shown to proceed via Volmer-Weber growth mode with dislocation being introduced in islands as small as 10 nm. The small InAs size for dislocation introduction pretty much precluded any possibility of using InAs SAQD on Si (001) for optoelectronic applications. In contrast to Ge SAQDs on Si, InAs islands do not show preferential nucleation when grown over a buried stressor. These results show that, despite of the vast volume of published literature, the physics of guided assembly via epitaxy

remains poorly understood and is therefore an exciting research area.

Acknowledgement

This work was supported by MARCO/FENA program.

References

- [1] H.J. Kim, Z.M. Zhao, Y.H. Xie, *Phys. Rev.*, B 68 (2003) 205312.
- [2] O.G. Schmidt, N.Y. Jin-Phillipp, C. Lange, U. Denker, K. Eberl, R. Schreiner, H. Gräbeldinger, H. Schweizer, *Appl. Phys. Lett.* 77 (2000) 4139.
- [3] T.I. Kamins, R. Stanley Williams, *Appl. Phys. Lett.* 71 (1997) 1201.
- [4] R.R. Li, P.D. Dapkus, M.E. Thompson, W.G. Jeong, C. Harrison, P.M. Chaikin, R.A. Register, D.H. Adamson, *Appl. Phys. Lett.* 76 (2000) 1689.
- [5] Z. Zhong, G. Bauer, *Appl. Phys. Lett.* 84 (2004) 1922.
- [6] B. Yang, F. Liu, M.G. Lagally, *Phys. Rev. Lett.* 92 (2004) 025502.
- [7] A.E. Romanov, P.M. Petroff, J.S. Speck, *Appl. Phys. Lett.* 74 (1999) 2280.
- [8] Y.H. Xie, G.H. Gilmer, C. Roland, P.J. Silverman, S.K. Buratto, J.Y. Cheng, E.A. Fitzgerald, A.R. Kortan, S. Schuppler, M.A. Marcus, P.H. Citrin, *Phys. Rev. Lett.* 73 (1994) 3006.
- [9] P. Mansky, Y. Liu, E. Huang, T.P. Russell, C. Hawker, *Science* 275 (1997) 1458.
- [10] H.J. Kim, Y.H. Xie, *Appl. Phys. Lett.* 79 (2001) 263.
- [11] S. Yu Shiryayev, F. Jensen, J.L. Hansen, J.W. Petersen, A.N. Larsen, *Phys. Rev. Lett.* 78 (1997) 503.
- [12] F.M. Ross, J. Tersoff, R.M. Tromp, *Phys. Rev. Lett.* 80 (1998) 984.
- [13] Y.H. Xie, S.B. Samavedam, M. Bulsara, T.A. Langdo, E.A. Fitzgerald, *Appl. Phys. Lett.* 71 (1997) 3567.
- [14] H.J. Kim, Z.M. Zhao, J. Liu, V. Ozolins, Y.H. Xie, *J. Appl. Phys.* 95 (2004) 6065.
- [15] L. Huang, F. Liu, X.G. Gong, *Phys. Rev.*, B 70 (2004) 155320.
- [16] C. Ratsch, M.F. Gyure, R.E. Caflisch, F. Gibou, M. Petersen, M. Kang, J. Garcia, D.D. Vvedensky, *Phys. Rev. B* 65 (2002) 195403.
- [17] T.I. Kamins, R.S. Williams, *Appl. Phys. Lett.* 71 (1997) 1201.
- [18] Z. Zhong, A. Halilovic, M. Mühlberger, F. Schäffler, G. Bauer, *J. Appl. Phys.* 93 (2003) 6258.
- [19] J.S. Kim, et al., *J. Appl. Phys.* 94 (2003) 6603, see, for example.